

Variability of manometric sea level from reanalyses and observation-based products over the Arctic and North Atlantic Oceans and the Mediterranean Sea

Andrea Storto¹, Giulia Chierici¹, Julia Pfeffer², Anne Barnoud², Romain Bourdalle-Badie³, Alejandro Blazquez⁴, Davide Cavaliere¹, Noémie Lalau², Benjamin Coupry², Marie Drevillon³, Sebastien Fourest⁴, Gilles Larnicol², Chunxue Yang¹

¹ Institute of Marine Sciences (ISMAR), National Research Council (CNR), Rome, Italy

² Magellium, 31520 Ramonville-Saint-Agne, France

³ Mercator Ocean International (MOI), 31400 Toulouse, France

10 ⁴ Laboratory of Space Geophysical and Oceanographic Studies (LEGOS), 31401 Toulouse, France

Correspondence to: Andrea Storto, Institute of Marine Sciences (ISMAR), National Research Council (CNR), via del Fosso del Cavaliere 100, I-00133 Roma, Italy; Email: andrea.storto@cnr.it

Abstract. Regional variations of the mass component of sea level (manometric sea level) are intimately linked with the changes in the water cycle, volume transports, and inter-basin exchanges. Here, we investigate the consistency at the regional level of the manometric sea level from the Copernicus Marine Service global reanalyses and compare with observation-based products, deduced from either gravimetry (GRACE missions) or altimetry and in-situ ocean observations (sea level budget approach, SLB), for some climate-relevant diagnostics such as interannual variability, trends, and seasonal amplitude. The analysis is performed for three basins (Mediterranean Sea; Arctic, and North Atlantic Oceans), and indicates very different characteristics across the three. The Mediterranean Sea exhibits the largest interannual variability, the Arctic Ocean the largest trends, and the North Atlantic a nearly linear increase that is well explained by global barystatic sea level variations. The three datasets show significant consistency at both the subannual and the interannual time scales, although differences in linear trends are sometimes significant (e.g., GRACE overestimates the trend in the Arctic and underestimates it in the Mediterranean Sea, compared to the other products). Furthermore, GRACE and GREP prove mutually more consistent than in comparison with SLB in most cases. Finally, we analyze the main modes of variability for the selected ocean basins and link them with large-scale modes of climate variability; the North Pacific Gyre Oscillation, the Arctic Oscillation, and the Atlantic Multidecadal Oscillation are proven to be the most influential modes for the North Atlantic Ocean, Mediterranean Sea, and Arctic Ocean manometric sea level, respectively.

Short summary. The variability of the manometric sea level (i.e., the sea level mass component) in three ocean basins is investigated in this study using three different techniques (reanalyses, gravimetry, and altimetry in combination with in-situ observations). We identify the emerging long-term signals, the consistency of the datasets, and the influence of large-scale climate modes on the regional manometric sea level variations at both subannual and interannual time scales.

1 Introduction

35 Contemporary changes in global sea level at the interannual timescale are driven mostly by two contributions: the changes in the density-driven variations of sea level, the so-called steric sea level that responds to the expansion and contraction of seawater due, mostly, to increasing heat in the oceans (Storto et al., 2019a). The other contributor to global sea level change is the ocean mass change, called barystatic sea level (Gregory et al., 2019). Barystatic sea level has been recently found to be responsible for the majority (about 60%) of the global sea level changes, (Frederikse et al., 2020; Fox-Kemper et al., 2021).
40 Recent estimates indicate $2.25 \pm 0.16 \text{ mm yr}^{-1}$ of sea level rise due to barystatic changes for the recent period (2005-2016) (Amin et al., 2020). Changes in barystatic sea level are due to the loss of mass from glaciers and ice sheets (Greenland and Antarctica) and changes in the global water cycle and land water storage. As such, barystatic sea level changes are a fundamental proxy of climate change and are expected to increase even more dramatically in the future, due to increased ice melting according to future projections (Oppenheimer et al., 2019).

45 At the regional scale, local dynamics, and regional hydrology, together with cross-basin exchanges, modulate regional ocean mass exchanges, called manometric sea level (Gregory et al., 2019). For instance, Camargo et al. (2022) show that regional trends in manometric sea level may vary from -0.4 to 3.3 mm yr^{-1} across the global ocean for the 2003-2016 period. Typically, regions characterized by high dynamic variability are characterized by large manometric variations. Strong climate modes of variability (e.g., the North Atlantic Oscillation) are also responsible for large deviations in manometric sea level (e.g., Criado-Aldeanueva et al., 2014; Volkov et al., 2019); fingerprinting techniques can be used to estimate the influence of a specific climate index on the resulting sea level variability (e.g., Pfeffer et al., 2022). In the Mediterranean Sea, for instance, variations are intimately linked to the exchanges with the Atlantic Ocean through the Gibraltar Strait, and variations in the atmospheric freshwater input, which are both strongly linked to North Atlantic variability (e.g., Tsimplis and Josey, 2001).

50 Since 2002, methods to observe and analyze manometric and barystatic sea level variations have generally relied on GRACE (Gravity Recovery And Climate Experiment; e.g. Tapley et al., 2004) and GRACE-FO (GRACE-Follow On; Landerer et al., 2020) satellite mission measurements of the temporal and spatial variations of the Earth's gravity field. Barystatic and manometric sea level signals can also be inferred from the difference between total sea level, measured by altimetry missions, and steric sea level, estimated through in-situ observations (e.g., Horwath et al., 2022). This approach will be referred to as the Sea Level Budget (SLB) method in the remainder of this article.

60 Alternatively, ocean general circulation model (OGCM) simulations embed the variability of sea level and its components, although they significantly lack realism (e.g., Kohl et al., 2007). Ocean reanalyses, which combine an ocean model with observations through data assimilation (Storto et al., 2019b) are in turn able to provide a good estimation of the sea level variability at global and basin scales (e.g., Storto et al., 2017); they are thus complementary to gravimetry based and sea level budget based observational counterparts and can be used for several investigations (e.g., Peralta-Ferriz et al., 2014; Marcos, 2015; Hughes et al., 2018). A few limitations in the use of reanalyses exist, though. First, the usual Boussinesq approximation in the OGCMs leads to a zero global steric sea level by construction, as the models cannot represent the global expansion and contraction in the constant volume framework. However, the global steric sea level can be computed and added to the model sea surface height retrospectively, since it does not have any dynamical signature (e.g., Greatbatch, 1994).

70 A more critical and long-standing issue in reanalyses regards the barystatic and manometric sea level components. Indeed, both the use of climatological freshwater input from land and ice and the imbalance of the atmospheric freshwater forcing combined with the evaporation and sublimation calculated by the ocean model make barystatic and manometric terms often unrealistic. Some reanalyses correct the barystatic sea level with globally uniform offsets, either time-varying or constant. In any case, the barystatic signal is generally unrealistic, and the manometric one may be affected by inaccuracies in the freshwater input into the oceans. In general, ocean bottom pressure data derived from gravimetry could also be directly
75 assimilated into ocean models (see e.g., Köhl et al., 2012). However, this approach was found suboptimal, mostly due to the

low signal-to-noise ratio of the gravimetry data compared to altimetry data assimilation (e.g., Storto et al., 2011), and their issues related to the pre-processing (persistent stripes and land water leakage). More recently, however, ingesting gravimetry data (e.g., in ECCOv4r4, ECCO Consortium, 2020) has proven promising to better capture high-frequency sea level variability (Schindelegger et al., 2021). Finally, the limited spatial resolution of the models may limit the representativeness of sea level variations in mesoscale active areas (e.g., Androsov et al., 2020).

The goal of this paper is manifold. First, we aim to estimate the consistency of manometric sea level from notably different approaches, which use numerical ocean models, gravimetry or altimetry, and in-situ observations. These approaches are known to contain different sources of uncertainty and none of them is fully trustable, as discussed in detail in this and the next sections. By doing so, we can rank the diagnostics, and areas, showing the largest consistency and, hence, confidence. Particular attention is devoted to assessing whether the latest generation of the Copernicus Marine Service global reanalyses can capture the interannual variations of the manometric sea level. Second, we aim at quantifying regional trends and amplitudes, to identify the emerging levels and scales of manometric sea level variability depending on the specific basin. Finally, we aim to fingerprint the manometric sea level with several climate mode indices, to connect such variations with large-scale climate variability.

The structure of the paper is as follows: we compare regionally (section 3) the manometric sea level from reanalyses with those coming from satellite gravimetry or the sea level budget approach (described in section 2). The exercise will therefore indicate the consistency of the reanalyses and observation-based products for selected metrics. Finally, we summarize and conclude (section 4).

2 Data and Methods

In this section, we shortly introduce the datasets used in the assessment. We refer to Gregory et al. (2019) for the terminology and definitions used to characterize the sea level components.

2.1 Gravimetry-based dataset

Barystatic and manometric sea level anomalies have been estimated from April 2002 to August 2022 at a monthly timescale and with a spatial resolution of 1° using an ensemble of GRACE and GRACE-FO solutions (Product ref. no. 2 in Table 1). The GRACE and GRACE-FO ensemble is constituted of 120 solutions, allowing us to estimate the uncertainties associated with different processing strategies and geophysical corrections needed for ocean applications. The ensemble is based on coefficients of the Earth's gravitational potential anomalies estimated by five different processing centers (CNES, CSR, JPL, GFZ, ITSG). A large variety of post-processing corrections are applied to the ensemble, including two geocenter motions (Lemoine and Reinquin, 2017; Sun et al., 2016), three oblateness values (C20) of the Earth (Cheng et al., 2013; Lemoine and Reinquin, 2017; Loomis et al., 2019), and two Glacial Isostatic Adjustment (GIA) corrections (Peltier et al., 2015, Caron et al., 2018). To reduce the anisotropic noise, characterized by typical stripes elongated in the North-South direction, decorrelation filters, called DDK filters (Kusche et al., 2009), are applied to GRACE solutions, using two different orders (DDK3 and DDK6) corresponding to different levels of filtering. The ensemble of 120 solutions results from the combination of these five processing centers, two geocenter models, three oblateness models, two GIA corrections, and two filters. The ensemble standard deviation provides a measure of uncertainty for both the barystatic and manometric sea level timeseries.

2.2 Sea level budget-based dataset

The estimation of barystatic and manometric sea level changes is extended to the altimetry era (January 1993 - December 2020) using the sea level budget approach (Product ref. no. 3 in Table 1). The manometric sea level changes are calculated as

115 the difference between the geocentric sea level changes based on satellite altimetry and steric sea level changes based on in situ measurements of the seawater temperature and salinity. The reliability of this dataset is intrinsically linked to the altimetry and in-situ observational sampling. Only within the global mean values, i.e. the barystatic sea level, changes are computed as the difference between the global mean geocentric sea level changes and thermosteric sea level changes to avoid drifts due to Argo salinity measurement errors (Barnoud et al., 2021; Wong et al., 2020); however, regional (manometric) sea level estimates include the halosteric contribution in the steric evaluation.

120 Geocentric sea level changes are estimated using the vDT2021 sea level product provided by the Copernicus Climate Change Service (C3S; Legeais et al., 2021). Geocentric sea level changes are corrected for the drifts in Topex-A altimeter (Ablain, 2017) and Jason-3 microwave radiometer wet troposphere correction (Barnoud et al., 2023a, 2023b), for the GIA effect, using the ensemble mean of 27 GIA models (Prandi et al., 2021) centered on ICE5G-VM2 (Peltier et al., 2004), and for the elastic deformation of the solid Earth due to present-day ice melting (Frederikse et al., 2017). The uncertainty of the geocentric sea level changes is calculated with the uncertainty budget and method detailed in Guérou et al. (2023) for the global mean sea level changes and in Prandi et al. (2021) for the local sea level changes.

130 Steric sea level changes are estimated as the sum of the thermosteric and halosteric sea level changes calculated from gridded temperature and salinity estimates from three different centers including EN4 (Good et al., 2013), IAP (Cheng et al., 2020) and Ishii et al. (2006). EN4 provides four datasets with different combinations of corrections for XBT and MBT measurements applied, leading to an ensemble of 6 temperature and salinity datasets. From these datasets, we compute the thermosteric and halosteric sea level changes due to temperature and salinity variations between 0 and 2000 m depth. The deep ocean contribution (i.e., below 2000 m) is considered only in the global barystatic signal and taken as a linear trend of 0.12 ± 0.03 mm yr⁻¹ (Chang et al., 2019) added to the time-varying steric sea level; for the regional estimates of the manometric sea level, the deep and abyssal ocean contribution is neglected, as there are not enough data for constraining it at regional level.

135 Steric sea level changes are estimated as the ensemble mean of the 6 solutions, and their uncertainties are estimated with the covariance matrix of the ensemble. The resulting barystatic and manometric uncertainties are described by the covariance matrix obtained by summing the sea level and steric covariance matrices.

2.3 The reanalysis dataset

140 In this work, we use the Global Reanalysis Ensemble Product (GREP) from the Copernicus Marine Service (Product ref. no. 1 in Table 1), which is a small-ensemble global reanalysis product, including in turn the four reanalyses i) CGLORS (v7) from CMCC; ii) GloSea5 from UKMO; iii) GLORYS2 (V4) from Mercator Ocean, and iv) ORAS5 from ECMWF. All reanalyses are performed using the NEMO ocean model (Madec et al., 2017) configured at about 1/4° of horizontal resolution and 75 levels. However, the four reanalyses differ for several issues, which can be summarized in the i) NEMO model version and a few selected parametrizations, including specific choice in the use of the ECMWF reanalysis (ERA-Interim and ERA5) atmospheric forcing; ii) initial conditions at the beginning of the reanalyzed period, which covers from 1993 to 2019 and is being updated in delayed time mode; iii) the data assimilation scheme, and iv) the set of observations assimilated, including their source and pre-processing procedures. Thus, GREP can span, to a good extent, the uncertainty linked with model physics and input datasets. We have used monthly mean data at 1/4° of horizontal resolution for the comparison described in the following section. More details of the four reanalyses together with some in-situ-based validation and assessment of the ensemble standard deviation are provided by Storto et al. (2019c).

150 The estimation approach for GREP follows that of the sea level budget approach (see section 2.2), where the manometric sea level is calculated as a difference from the total sea surface height anomaly from the reanalysis, and the steric sea level anomaly, calculated from the reanalysis output temperature and salinity fields. Thus, we can cross-compare GREP data with GRACE and SLB datasets in terms of interannual variability, trend, and seasonal amplitude.

Basin-averaged timeseries are analyzed in the next section as monthly means to assess the main variability signal over three oceanic basins (the Arctic Ocean, defined as the region covering from 67°N in the Atlantic to the Bering Strait; the North Atlantic Ocean, defined from 0°N to 67°N; the Mediterranean Sea). Timeseries are also analyzed in terms of their interannual and subannual signal, where the interannual signal is the timeseries to which the monthly climatology has been subtracted, and the subannual the residual part. The uncertainty of the timeseries corresponds to that provided by the dataset (which in turn uses an ensemble approach to estimate uncertainty as ensemble standard deviation); by construction, GREP, with only four members, is known to underestimate the uncertainty of sea level (Storto et al., 2019c). Uncertainty of trends is estimated through bootstrapping (Efron, 1979) and closely resembles the estimates calculated following Storto et al. (2022). The Bootstrapping technique randomly removes part of the timeseries, and thus quantifies the sensitivity of the trend to individual years and periods. Explained variance is used to quantify how much of the regional signal is explained by the global barostatic signal due to fast barotropic motion. For this analysis, we use only global GRACE and SLB timeseries and show only SLB for the sake of clarity (see, e.g. Barnoud et al., 2023b, for a discussion on their comparison), because the GREP barostatic sea level is either unreliable due to drifts in the freshwater forcing, or it is adjusted to GRACE-derived data and, thus, is not independent. Seasonal amplitude is defined by fitting the monthly data to a sinusoidal curve, while interannual variability is the standard deviation of the detrended and de-seasonalized timeseries. Percents of manometric sea level trends over the total sea level ones are calculated from the Copernicus Marine Service dataset (Product ref. no. 4 in Table 1), over each region. LASSO regression (Tibshirani, 1997), performed between the normalized manometric sea level and normalized climate indices, is a regularization technique for multivariate regression, which is used in this study to rank the influence of the climate indices on the basin-averaged manometric sea level, in a way similar to what Pfeffer et al. (2022) proposed. Like the latter and previous studies, raw monthly means were used without low-pass filtering the data, which could induce arbitrary preferences in the regression within our multi-variate analysis. After performing k-fold cross-validation (with 10 folds) to identify the best hyperparameters, LASSO regression avoids overfitting the regression, such that absolute values of the regression coefficients quantify the impact of a predictor on the manometric sea level. We also verified that other methods (e.g., the R^2 hierarchical decomposition from Chevan and Sutherland, 1991) provide the same results. For these analyses, the *glmnet* (Friedman et al., 2010) and *relaimpo* (Groemping, 2006) R packages are used. Finally, for the statistical significance of the correlations and their differences, we used the *psych* R package (Revelle, 2023) that implements Steiger's test for comparing dependent correlations (Steiger, 1980; Olkin and Finn, 1995). All statistical significance results are provided at the 99% confidence level.

3 Results

We present the results of the assessment, by first analyzing the timeseries and several diagnostics of the basin-averaged manometric sea level. Then, the consistency between the manometric sea level products is addressed; finally, the influence of the climate modes of variability on the manometric sea level variability is analyzed.

3.1 Manometric sea level timeseries

The monthly means of the manometric sea level for the three basins considered in this study is shown in Figure 1, while several diagnostics (trend, seasonal amplitude, interannual variability, and mean uncertainty) are provided in Table 2, for the three datasets considered.

The three basins (Arctic Ocean, North Atlantic Ocean, and Mediterranean Sea) exhibit different behavior; GRACE, SLB, and GREP show, however, qualitatively good consistency in all three seas. The Arctic Ocean has a regular periodicity and a large seasonal amplitude, with a generally increasing yearly mean signal, except during the first years of the timeseries (2003-2005).

195 For both GRACE and GREP, the latest years are the ones with the largest manometric sea level, which is reflected in large trends (2.45 ± 0.44 and 3.45 ± 0.57 mm yr⁻¹, respectively) compared to the other seas, while SLB shows a weaker trend. Changes in manometric sea level changes at interannual time scales are very different over the Arctic Ocean than the global ocean (Table 3), meaning that internal dynamics, straits connections, and the sea-ice seasonal cycle significantly modulate the regional manometric sea level. Sub-annual timeseries are more largely explained by the global signal for both datasets (38-48%).

200 The North Atlantic manometric sea level signal has a seasonality (10 to 14 mm, depending on the dataset), smaller than the other basins, the smallest interannual variability (6.6 to 8.6 mm), and a nearly linearly increasing mean signal that dominates the variability. The percent variance explained by the global barystatic sea level is large (71% and 79% for GRACE and SLB, respectively, for the interannual signal), meaning that, as expected, the North Atlantic resembles largely the global signal. Here, the trend accounts for about 60-80% of the total sea level trend, depending on the specific product used.

205 In the Mediterranean Sea, the interannual variability is the largest (more than 25 mm for all datasets) and does not follow the global barystatic signal (see the low percent explained variance in Table 3, especially for the interannual signal, no matter which dataset is considered). This suggests that the regional water cycle and sea level budget are mostly independent of the global one, and this is ascribed to the role of Gibraltar Strait (see e.g., Landerer and Volkov, 2013). Trends in the Mediterranean Sea are generally lower than in the other basins and explain about 40%, on average, of the total sea level trend from altimetry.

210 All the datasets exhibit the largest trends in the western part of the Mediterranean Sea (not shown), although with slightly different patterns. Remarkable peaks of the manometric sea level are visible in 2006, 2010, 2011, and 2018; for these events, GREP tends to underestimate the maxima compared to the other two datasets.

In terms of the uncertainty (see Table 2 and Figure 1), the GRACE dataset exhibits the largest mean uncertainty (about 30 mm in all basins), while the uncertainty of SLB ranges from about 12 mm in the Arctic Ocean and the Mediterranean Sea to about 21 mm in the North Atlantic Ocean. GREP uncertainty is the lowest, except in the Mediterranean Sea where it is comparable to SLB. However, the uncertainty estimates are strongly affected by the ensemble size, which is substantially different across the three datasets (see section 2). Besides, common errors, associated for example with spatial under-sampling, which may be large for the SLB method, will be neglected with the ensemble approach.

215

3.2 Consistency between timeseries

220 The consistency between the three timeseries is investigated by decomposing the full signal in the interannual and subannual timeseries. The correlation matrix for the three temporal scales and the three basins is shown in Figure 2.

In the North Atlantic Ocean and the Mediterranean Sea, the largest correlations are generally between SLB and GREP. SLB and GREP are not independent due to the use of altimetry and in-situ observations in both, so this result likely reflects their dependency. At the interannual timescale, the correlation between GRACE and SLB is slightly larger (but the difference is not statistically significant) than that between GRACE and GREP, suggesting that for these regions SLB might capture the year-to-year variations better than the reanalyses. At the subannual scale in the Mediterranean Sea, however, the consistency between GRACE and GREP is larger than that between GRACE and SLB (with a statistically significant difference), suggesting that the reanalyses capture the seasonal cycle better than SLB with respect to gravimetry data. For both regions, the high consistency of manometric sea level from reanalyses compared to the two observation-based datasets suggests the good reliability of the GREP ensemble mean in capturing the sea level variations.

230 In the Arctic Ocean, a large consistency is found between GRACE and GREP; the correlations involving SLB are statistically significantly lower than the others, at all time scales (full, inter and subannual) at the 99% confidence level; this is also visible, in Figure 1, as fluctuations of the SLB timeseries not reproduced by the other two datasets. This suggests that in the Arctic Ocean, gravimetry and reanalyses are largely consistent, and their use should be preferred, while the poor quality of in-situ observational sampling compromises the SLB reliability. On the one hand, the meridional transports, sea-ice modeling, and

235

atmospheric forcing, implicit in the reanalysis systems, are known to be able to shape the Arctic Ocean interannual variability realistically (see e.g. Mayer et al., 2016; 2019); on the other hand, altimetry and in-situ data are poorly sampled in the Arctic Ocean, making more challenging to apply the SLB approach therein.

3.3 Influence of climate indices on manometric sea level variations

240 Several climate indices are considered predictors for the manometric sea level in the three basins (Arctic Ocean, North Atlantic Ocean, and Mediterranean Sea). Their acronyms and meanings are listed in the caption of Figure 3. The detailed justification for inclusion in the analysis is provided by Pfeffer et al. (2022): through representing well-determined atmospheric circulation regimes, the indices synthesize the water cycle and the atmospheric forcing variability regimes, leading in turn to variations in the regional manometric sea level due to changes in oceanic divergence and freshwater forcing. For instance, the El Niño Southern Oscillation (ENSO) has a prominent role in modifying precipitation patterns, with obvious implications on the manometric sea level (e.g., Muis et al., 2018); changes in the North Atlantic Oscillation (NAO) modify atmospheric and oceanic transports in North America and Europe, implying changes also in the Mediterranean Sea through modification to exchanges at Gibraltar and precipitation patterns (Landerer et al., 2013; Storto et al., 2019a). It is beyond the scope of this study to explain all possible modes of co-variability and the interested readers are referred to the specific literature for a broad overview (e.g., Andrew et al., 2006; Peralta-Ferriz et al., 2014; Merrifield et al., 2018; Volkov et al., 2019; Pfeffer et al., 2022). Raw monthly means of manometric sea level are used in this study, to avoid arbitrary filtering affecting the regression results; the climate indices, however, are used with filtering as in their standard definition.

In the Arctic Ocean, the largest influence is found to be due to the Atlantic Multidecadal Oscillation (AMO), with values ranging from 25 to 35% depending on the dataset. AMO is known to modulate the sea-ice interannual variations and the Arctic amplification (Li et al., 2018; Fang et al., 2022), which are both important contributors to the sea level manometric fluctuations. IOD, NAO, and NPGO also significantly affect the Arctic manometric sea level, although the consensus between the datasets varies, and the influence of the IOD is questionable. The Arctic Oscillation is found influential when using the GRACE dataset consistently with previous studies (Peralta-Ferriz et al., 2014), although the other datasets show, in general, other preferences. The North Atlantic manometric sea level is characterized by the largest impact of NPGO, consistently across all the datasets. While NPGO well explains variations in the eastern North Pacific Ocean (Di Lorenzo et al., 2008), its impact on the North Atlantic manometric sea level likely depends on the global barystatic signal and teleconnections (Iglesias et al., 2018). NPGO accounts for more than 25% of the North Atlantic manometric sea level variability, peaking at more than 40% for the SLB dataset. Significant impact in the North Atlantic manometric sea level is also given by variations described by the PDO, AMO, and IOD, although for the latter small consistency is found across the datasets.

260 Finally, in the Mediterranean Sea, the largest influence is provided by the Arctic Oscillation (AO), which explains more than 30% of the manometric sea level covariations for all datasets. AO is an expression of the North Atlantic variability, strictly linked to the NAO and closely linked to the North European wind circulation (e.g., Ambaum et al., 2001); while these are strictly connected, the regularization technique used here clearly indicates AO as a better predictor than NAO for the regional manometric sea level. Other influential climate modes of variability are linked to the North Pacific variability, namely the PDO and NPGO.

4. Summary and Discussion

In this study, we have focused on the basin-averaged manometric sea level for a few regional basins (Arctic Ocean, North Atlantic Ocean, Mediterranean Sea) and from different datasets, to investigate the consistency, the emerging climate signals, the differences between the basin characteristics, and the link with the main large-scale modes of variability. These three basins

275 were chosen as part of the focus of the EU Copernicus Marine Service and are large enough to be resolved at basin scale by the observing and modeling systems used herein, unlike other smaller basins.

To the authors' knowledge, it is the first time that different datasets of manometric sea level from reanalyses, gravimetry, and altimetry minus in-situ data, are compared at the regional level to infer their strengths and weaknesses. The three basins (Arctic Ocean, North Atlantic Ocean, Mediterranean Sea) exhibit inherently different features, with the Mediterranean Sea showing, on average over the three products, the largest interannual variability, and the smallest trends; the Arctic Ocean shows large seasonal amplitude and the largest trend, and the North Atlantic Ocean a quasi-linear trend, which is very well explained by the global barostatic signal. The three products are found in reasonable agreement, with all pairs significantly correlated at both inter- and subannual time scales. There are, however, non-negligible differences in the quantitative assessment; for instance, GRACE leads to a large trend in the Arctic basin ($3.45 \pm 0.57 \text{ mm yr}^{-1}$), which is not reproduced by either GREP or SLB and needs to be investigated in more detail; or a trend in the Mediterranean Sea smaller than the others.

In the Arctic Ocean, altimetry minus in-situ (SLB) is generally less in agreement with the other datasets based on correlation scores; this might be due to the poor altimetry and in-situ sampling, on which the SLB approach is based (see the PUM, Table 1), which could be alleviated in reanalyses, to some extent, by the atmospheric forcing information and the meridional exchanges. In the Mediterranean Sea, subannual scale agreement is also the largest between GRACE and GREP, suggesting in turn that the Copernicus Marine Service global reanalyses can capture the manometric sea level variability in the studied regions.

Finally, a fingerprinting technique based on regularization in regression is used to quantify the influence of several large-scale climate modes of variability on the basin-averaged manometric sea level. In most cases, we found consistency in the results using the three different datasets. The analysis indicates the NPGO (North Pacific Gyre Oscillation), AO (Arctic Oscillation), and AMO (Atlantic Multidecadal Oscillation) to be the most influential modes for the North Atlantic Ocean, Mediterranean Sea, and Arctic Ocean, respectively. This is the combined result of teleconnection patterns and cross-basin exchanges, as explained in detail in previous studies (Landerer and Volkov, 2013; Iglesias et al., 2018; Fang et al., 2022). These results are useful as a reference for further fingerprinting technique applications and as a possible tool for statistical prediction of manometric variations.

These results provide a summary of the manometric sea level variability within the three basins investigated here and guide users in the choice of the specific product, depending on the region of interest. The overarching conclusions are that reanalyses when an ensemble mean of different systems is adopted, provide good performances in all basins; SLB performance is the most affected by observational sampling, and thus should be avoided in regions with poorly developed networks; gravimetry data provide realistic sub-seasonal and interannual variability, although long-term trends are less consistent than other datasets and the monthly uncertainty is the largest.

Further studies are needed to understand the different behavior of the datasets for certain aspects (e.g., the over-estimation of the Arctic Ocean manometric sea level trend by GRACE, or its under-estimation in the Mediterranean Sea), namely whether this is due to some intrinsic limitations of the data processing, or the different processes implied by the measurement techniques.

Data availability
See Table 1 for accessing the data through the associated DOI.

Author contribution
AS designed the analysis and wrote most of the text; GC and AS performed the analysis; JP coordinated the processing of the manometric sea level data from GRACE, revised the manuscript, and provided many comments on the use of the observation-

based datasets and the fingerprinting technique; AB corrected in detail the Data and methods section; all authors contributed with data production and suggestions for improving the study.

320

The authors declare no competing interests.

Acknowledgments

325

The authors thank the OSR8 team (Karina von Schuckmann and Lorena Moreira Mendez) for their coordination efforts and suggestions to improve the quality of the original version of the manuscript. This work has been supported by the GLORAN-Lot8 and the WAMBOR contracts of the Copernicus Marine Service.

References

- 330 Ablain, M., Legeais, J. F., Prandi, P., Marcos, M., Fenoglio-Marc, L., Dieng, H. B., ... Cazenave, A. (2017). Satellite altimetry-based sea level at global and regional scales. *Surveys in Geophysics*, 38, 7–31.
- Ambaum, M. H. P., B. J. Hoskins, and D. B. Stephenson, 2001: Arctic Oscillation or North Atlantic Oscillation?. *J. Climate*, 14, 3495–3507, [https://doi.org/10.1175/1520-0442\(2001\)014<3495:AONAO>2.0.CO;2](https://doi.org/10.1175/1520-0442(2001)014<3495:AONAO>2.0.CO;2).
- Amin, H.; Bagherbandi, M.; Sjöberg, L.E. Quantifying barystatic sea-level change from satellite altimetry, GRACE and Argo observations over 2005–2016. *Adv. Space Res.* 2020, 65, 1922–1940.
- 335 Andrew, J.A.M., Leach, H. & Woodworth, P.L. The relationships between tropical Atlantic sea level variability and major climate indices. *Ocean Dynamics* 56, 452–463 (2006). <https://doi.org/10.1007/s10236-006-0068-z>
- Androsov, A., Boebel, O., Schröter, J., Danilov, S., Macrander, A., & Ivanciu, I. (2020). Ocean bottom pressure variability: Can it be reliably modeled? *Journal of Geophysical Research: Oceans*, 125, e2019JC015469. <https://doi.org/10.1029/2019JC015469>
- 340 Barnoud, A., Pfeffer, J., Guérou, A., Frery, M.-L., Siméon, M., Cazenave, A., Chen, J., Llovel, W., Thierry, V., Legeais, J.-F., and Ablain, M.: Contributions of altimetry and Argo to non-closure of the global mean sea level budget since 2016, *Geophysical Research Letters*, 48, e2021GL092824, <https://doi.org/10.1029/2021gl092824>, 2021.
- Barnoud, A., Picard, B., Meyssignac, B., Marti, F., Ablain, M., & Roca, R. (2023a). Reducing the uncertainty in the satellite altimetry estimates of global mean sea level trends using highly stable water vapor climate data records. *Journal of Geophysical Research: Oceans*, 128, e2022JC019378. <https://doi.org/10.1029/2022JC019378>
- 345 Barnoud, A., Pfeffer, J., Cazenave, A., Fraudeau, R., Rousseau, V., and Ablain, M. (2023b). Revisiting the global mean ocean mass budget over 2005–2020, *Ocean Sci.*, 19, 321–334, <https://doi.org/10.5194/os-19-321-2023>
- Camargo, C. M. L., Riva, R. E. M., Hermans, T. H. J., and Slangen, A. B. A.: Trends and uncertainties of mass-driven sea-level change in the satellite altimetry era, *Earth Syst. Dynam.*, 13, 1351–1375, <https://doi.org/10.5194/esd-13-1351-2022>,
- 350 2022.
- Caron, L., Ivins, E., Larour, E., Adhikari, S., Nilsson, J. & Blewitt, G., 2018. GIA model statistics for GRACE hydrology, cryosphere, and ocean science, *Geophys. Res. Lett.*, 45(5), 2203–2212.
- Chambers, D. P. (2006), Evaluation of new GRACE time-variable gravity data over the ocean, *Geophys. Res. Lett.*, 33, L17603, doi:10.1029/2006GL027296.
- 355 Chang, L., Tang, H., Wang, Q., and Sun, W.: Global thermosteric sea level change contributed by the deep ocean below 2000 m estimated by Argo and CTD data, *Earth Planet. Sc. Lett.*, 524, 115727, <https://doi.org/10.1016/j.epsl.2019.115727>, 2019.
- Cheng M., Tapley B.D., Ries J.C., 2013. Deceleration in the Earth's oblateness, *J. geophys. Res.*, 118(2), 740–747, doi:10.1002/jgrb.50058
- Criado-Aldeanueva, F.; Soto-Navarro, F.J.; García-Lafuente, J. Large-scale atmospheric forcing influencing the long-term variability of Mediterranean heat and freshwater budgets: Climatic indices. *J. Hydrometeorol.* 2014, 15, 650–663.
- 360 Cheng, L., and Coauthors, 2020: Improved Estimates of Changes in Upper Ocean Salinity and the Hydrological Cycle. *J. Climate*, 33, 10357–10381, <https://doi.org/10.1175/JCLI-D-20-0366.1>.
- Chevan, A. and Sutherland, M. (1991) Hierarchical Partitioning. *The American Statistician* 45, 90-96.
- Desportes, C., Garric, G., Régnier, C., Drévilion, M., Parent, L., Drillet, Y., Masina, S., Storto, A., Mirouze, I., Cipollone, A.,
- 365 Zuo, H., Balmaseda, M., Peterson, D., Wood, R., Jackson, L., Mulet, S., Grenier, E., Gounou, A.: EU Copernicus Marine Service Quality Information Document for the Global Ocean Ensemble Physics Reanalysis, GLOBAL_REANALYSIS_PHY_001_031, Issue 1.1, Mercator Ocean International, <https://catalogue.marine.copernicus.eu/documents/QUID/CMEMS-GLO-QUID-001-031.pdf>, (last access: 24 July 2023), 2022

- 370 Di Lorenzo, E., et al. (2008), North Pacific Gyre Oscillation links ocean climate and ecosystem change, *Geophys. Res. Lett.*, 35, L08607, doi:10.1029/2007GL032838.
- ECCO Consortium, Fukumori, I., Wang, O., Fenty, I., Forget, G., Heimbach, P., & Ponte, R. M. (2020). Synopsis of the ECCO central production global ocean and sea-ice state estimate (version 4 release 4). Retrieved from https://ecco-group.org/docs/v4r4_synopsis.pdf Accessed 7 August 2020.
- 375 Efron, B. (1979). Bootstrap methods: Another look at the jackknife. *The Annals of Statistics*. 7 (1): 1–26. doi:10.1214/aos/1176344552
- EU Copernicus Marine Service Product: Global Ocean Ensemble Physics Reanalysis, Mercator Ocean International, [data set], <https://doi.org/10.48670/moi-00024>, 2022a
- EU Copernicus Marine Service Product: Global Ocean Gridded L 4 Sea Surface Heights And Derived Variables Reprocessed 1993 Ongoing, Mercator Ocean International, [data set], <https://doi.org/10.48670/moi-00148>, 2022b
- 380 Fang, M., Li, X., Chen, H.W. et al. Arctic amplification modulated by Atlantic Multidecadal Oscillation and greenhouse forcing on multidecadal to century scales. *Nat Commun* 13, 1865 (2022). <https://doi.org/10.1038/s41467-022-29523-x>
- Fox-Kemper, B., Hewitt, H. T., Xiao, C., Aðalgeirsdóttir, G., Drijfhout, S. S., Edwards, T. L., N. R. Golledge, M. H., Kopp, R. E., Krinner, G., Mix, A., Notz, D., Nowicki, S., Nurhati, I. S., Ruiz, L., Sallée, J.-B., Slangen, A. B. A., and Yu, Y.: Ocean, 385 Cryosphere and Sea Level Change, in: *Climate Change 2021: The Physical Science Basis. Contribution of Working Group I to the Sixth Assessment Report of the Intergovernmental Panel on Climate Change*, edited by: Masson-Delmotte, V., Zhai, P., Pirani, A., Connors, S. L., Péan, C., Berger, S., Caud, N., Chen, Y., Goldfarb, L., Gomis, M. I., Huang, M., Leitzell, K., Lonnoy, E., Matthews, J. B. R., Maycock, T. K., Waterfield, T., Yelekçi, O., Yu, R., and Zhou B., Cambridge University Press, Cambridge, United Kingdom and New York, NY, USA, 1211–1362 pp., <https://doi.org/10.1017/9781009157896.011>, 2021
- 390 Frederikse, T., Riva, R. E. M., & King, M. A. (2017). Ocean bottom deformation due to present-day mass redistribution and its impact on sea level observations. *Geophysical Research Letters*, 44, 12,306– 12,314. <https://doi.org/10.1002/2017GL075419>
- Frederikse, T., Landerer, F., Caron, L., Adhikari, S., Parkes, D., Humphrey, V. W., Dangendorf, S., Hogarth, P., Zanna, L., Cheng, L., and Wu, Y. H.: The causes of sea-level rise since 1900, *Nature*, 584, 393–397, [https://doi.org/10.1038/s41586-020-](https://doi.org/10.1038/s41586-020-2591-3) 395 [2591-3](https://doi.org/10.1038/s41586-020-2591-3), 2020.
- Friedman, J. H., Hastie, T., & Tibshirani, R. (2010). Regularization Paths for Generalized Linear Models via Coordinate Descent. *Journal of Statistical Software*, 33(1), 1–22. <https://doi.org/10.18637/jss.v033.i01>
- Good, S. A., M. J. Martin and N. A. Rayner, 2013. EN4: quality controlled ocean temperature and salinity profiles and monthly objective analyses with uncertainty estimates, *Journal of Geophysical Research: Oceans*, 118, 6704–6716, 400 doi:10.1002/2013JC009067
- Gounou, A., Drevillon, M., Clavier, M.: EU Copernicus Marine Service Product User Manual for the Global Ocean Ensemble Physics Reanalysis, GLOBAL_REANALYSIS_PHY_001_031, Issue 1.1, Mercator Ocean International, <https://catalogue.marine.copernicus.eu/documents/PUM/CMEMS-GLO-PUM-001-031.pdf>, (last access: 24 July 2023), 2022
- Greatbatch, R. J. (1994), A note on the representation of steric sea level in models that conserve volume rather than mass, *J. Geophys. Res.*, 99 (C6), 12767– 12771, doi:10.1029/94JC00847. 405
- Gregory, J. M., Griffies, S. M., Hughes, C. W., Lowe, J. A., Church, J. A., Fukimori, I., Gomez, N., Kopp, R. E., Landerer, F., Cozannet, G. L., Ponte, R. M., Stammer, D., Tamisiea, M. E., and van de Wal, R. S.: Concepts and Terminology for Sea Level: Mean, Variability and Change, Both Local and Global, *Surv. Geophys.*, 40, 1251–1289, [https://doi.org/10.1007/s10712-019-](https://doi.org/10.1007/s10712-019-09525-z) 410 [09525-z](https://doi.org/10.1007/s10712-019-09525-z), 2019
- Groemping, U. (2006). Relative Importance for Linear Regression in R: The Package relaimpo. *Journal of Statistical Software*, 17(1), 1–27. <https://doi.org/10.18637/jss.v017.i01>

- Guérou, A., Meyssignac, B., Prandi, P., Ablain, M., Ribes, A. and Bignalet-Cazalet, F. (2023). Current observed global mean sea level rise and acceleration estimated from satellite altimetry and the associated measurement uncertainty. *Ocean Science*, 19, 431-451. <https://doi.org/10.5194/os-19-431-2023>.
- 415 Horwath, M., Gutknecht, B. D., Cazenave, A., Palanisamy, H. K., Marti, F., Marzeion, B., Paul, F., Le Bris, R., Hogg, A. E., Otosaka, I., Shepherd, A., Döll, P., Cáceres, D., Müller Schmied, H., Johannessen, J. A., Nilsen, J. E. Ø., Raj, R. P., Forsberg, R., Sandberg Sørensen, L., Barletta, V. R., Simonsen, S. B., Knudsen, P., Andersen, O. B., Ranndal, H., Rose, S. K., Merchant, C. J., Macintosh, C. R., von Schuckmann, K., Novotny, K., Groh, A., Restano, M., and Benveniste, J.: Global sea-level budget and ocean-mass budget, with a focus on advanced data products and uncertainty characterisation, *Earth Syst. Sci. Data*, 14, 411–447, <https://doi.org/10.5194/essd-14-411-2022>, 2022.
- 420 Hughes, C. W., Williams, J., Blaker, A., Coward, A., & Stepanov, V. (2018). A window on the deep ocean: The special value of ocean bottom pressure for monitoring the large-scale, deep-ocean circulation. *Progress in Oceanography*, 161, 19– 46. <https://doi.org/10.1016/j.pocean.2018.01.011>
- Iglesias, I.; Lorenzo, M.N.; Lázaro, C.; Fernandes, M.J.; Bastos, L. Sea level anomaly in the North Atlantic and seas around Europe: Long-term variability and response to North Atlantic teleconnection patterns. *Sci. Total Environ.* 2017, 609, 861–874.
- 425 Ishii, M.; Kimoto, M.; Sakamoto, K.; Iwasaki, S.I. Steric sea level changes estimated from historical ocean subsurface temperature and salinity analyses. *J. Oceanogr.* 2006, 62, 155–170.
- Kohl, A.; Stammer, D.; Cornuelle, B. Interannual to Decadal Changes in the ECCO Global Synthesis. *J. Phys. Oceanogr.* 2007, 37, 313–337.
- 430 Köhl, A., Siegismund, F., and Stammer, D. (2012), Impact of assimilating bottom pressure anomalies from GRACE on ocean circulation estimates, *J. Geophys. Res.*, 117, C04032, doi:10.1029/2011JC007623.
- Kusche, J., Schmidt, R., Petrovic, S. et al. Decorrelated GRACE time-variable gravity solutions by GFZ, and their validation using a hydrological model. *J Geod* 83, 903–913 (2009). <https://doi.org/10.1007/s00190-009-0308-3>
- Landerer, F. W., and Volkov, D. L. (2013), The anatomy of recent large sea level fluctuations in the Mediterranean Sea, *Geophys. Res. Lett.*, 40, 553– 557, doi:10.1002/grl.50140.
- 435 Landerer, F.W., Flechtner, F.M., Save, H., Webb, F.H., Bandikova, T., Bertiger, W.I., Bettadpur, S.V., Byun, S.H., Dahle, C., Dobslaw, H. and Fahnestock, E., 2020. Extending the global mass change data record: GRACE Follow-On instrument and science data performance. *Geophysical Research Letters*, 47(12), p.e2020GL088306.<https://doi.org/10.1029/2020GL088306>
- Legeais J-F, Meyssignac B, Faugère Y, Guerou A, Ablain M, Pujol M-I, Dufau C and Dibarboure G (2021) Copernicus Sea Level Space Observations: A Basis for Assessing Mitigation and Developing Adaptation Strategies to Sea Level Rise. *Front. Mar. Sci.* 8:704721. doi: 10.3389/fmars.2021.704721
- 440 Lemoine, J.-M. and Reinquin, F. (2017). Processing of SLR Observations at CNES. Newsletter EGSIEM, pages 3.
- Li, F., Orsolini, Y. J., Wang, H., Gao, Y., & He, S. (2018). Atlantic multidecadal oscillation modulates the impacts of Arctic sea ice decline. *Geophysical Research Letters*, 45, 2497– 2506. <https://doi.org/10.1002/2017GL076210>
- 445 Loomis, B. D., Rachlin, K. E., & Luthcke, S. B. (2019). Improved Earth oblateness rate reveals increased ice sheet losses and mass-driven sea level rise. *Geophysical Research Letters*, 46, 6910– 6917. <https://doi.org/10.1029/2019GL082929>
- Madec G., The NEMO System Team (2017). NEMO ocean engine. note Du pole de modélisation (Paris, France: Institut Pierre-Simon Laplace). doi: 10.5281/zenodo.3248739/10.5281
- 450 Magellium et al., 2023. Barystatic and manometric sea level changes from satellite geodesy. AVISO/ODATIS webpage and doi in preparation.
- Marcos, M. Ocean bottom pressure variability in the Mediterranean Sea and its relationship with sea level from a numerical mode. *Global Planet. Change* 124, 10–21 (2015).
- Mayer, M., Haimberger, L., Pietschnig, M., and Storto, A. (2016), Facets of Arctic energy accumulation based on observations and reanalyses 2000–2015, *Geophys. Res. Lett.*, 43, 10,420– 10,429, doi:10.1002/2016GL070557.

- 455 Mayer, M., S. Tietsche, L. Haimberger, T. Tsubouchi, J. Mayer, and H. Zuo, 2019: An Improved Estimate of the Coupled Arctic Energy Budget. *J. Climate*, 32, 7915–7934, <https://doi.org/10.1175/JCLI-D-19-0233.1>.
- Merrifield, M.A.; Thompson, P.R. Interdecadal sea level variations in the Pacific: Distinctions between the tropics and extratropics. *Geophys. Res. Lett.* 2018, 45, 6604–6610.
- Muis, S., Haigh, I. D., Guimarães Nobre, G., Aerts, J. C. J. H., & Ward, P. J. (2018). Influence of El Niño–Southern Oscillation on global coastal flooding. *Earth's Future*, 6, 1311–1322. <https://doi.org/10.1029/2018EF000909>
- 460 Olkin, I., and Finn, J. D. (1995). Correlations redux. *Psychological Bulletin*, 118(1), 155–164. <https://doi.org/10.1037/0033-2909.118.1.155>
- Oppenheimer, M., Abdelgawad, A., Hay, J., Glavovic, B., Cai, R., Marzeion, B., Hinkel, J., Cifuentes-Jara, M., Meyssignac, B., Van De Wal, R., DeConto, R., Sebesvari, Z., Maignan, A., and Ghosh, Hay, T. J., Isla, F., Marzeion, B., Meyssignac, B., and Sebesvari, Z.: Sea Level Rise and Implications for Low-Lying Islands, Coasts and Communities, in: IPCC Special Report on the Ocean and Cryosphere in a Changing Climate, edited by: Pörtner, H.-O., Roberts, D. C., Masson-Delmotte, V., Zhai, P., Tignor, M., Poloczanska, E., Mintenbeck, K., Alegría, A., Nicolai, M., Okem, A., Petzold, J., Rama, B., Weyer, N. M., Cambridge University Press, Cambridge, UK and New York, NY, USA, 321–445, <https://doi.org/10.1017/9781009157964.006>, 2019.
- 465 Peltier, W.R., Argus, D.F. & Drummond, R., 2015. Space geodesy constrains ice age terminal deglaciation: the global ICE-6GC (VM5a) model, *J. Geophys. Res.*, 120(1), 450–487.
- Peltier, W. R.. GLOBAL GLACIAL ISOSTASY AND THE SURFACE OF THE ICE-AGE EARTH: The ICE-5G (VM2) Model and GRACE, *Annual Review of Earth and Planetary Sciences* 2004 32:1, 111-149
- Peralta-Ferriz, C., J. H. Morison, J. M. Wallace, J. A. Bonin, and J. Zhang, 2014: Arctic Ocean Circulation Patterns Revealed by GRACE. *J. Climate*, 27, 1445–1468, <https://doi.org/10.1175/JCLI-D-13-00013.1>.
- 475 Pfeffer, J., Cazenave, A. & Barnoud, A. Analysis of the interannual variability in satellite gravity solutions: detection of climate modes fingerprints in water mass displacements across continents and oceans. *Clim Dyn* 58, 1065–1084 (2022). <https://doi.org/10.1007/s00382-021-05953-z>
- Prandi, P., Meyssignac, B., Ablain, M. et al. Local sea level trends, accelerations and uncertainties over 1993–2019. *Sci Data* 8, 1 (2021). <https://doi.org/10.1038/s41597-020-00786-7>
- 480 Storto, A., Masina, S., Balmaseda, M. et al. Steric sea level variability (1993–2010) in an ensemble of ocean reanalyses and objective analyses. *Clim Dyn* 49, 709–729 (2017). <https://doi.org/10.1007/s00382-015-2554-9>
- Pujol: EU Copernicus Marine Service Product User Manual for the For Sea Level Altimeter products, Issue 7.0, Mercator Ocean International, <https://catalogue.marine.copernicus.eu/documents/PUM/CMEMS-SL-PUM-008-032-068.pdf>, (last access: 24 July 2023), 2022
- 485 Pujol, M.-I., G. Taburet and SL-TAC team. : EU Copernicus Marine Service Quality Information Document for the Sea Level TAC - DUACS products, Issue 8.2, Mercator Ocean International, <https://catalogue.marine.copernicus.eu/documents/QUID/CMEMS-SL-QUID-008-032-068.pdf>, (last access: 24 July 2023), 2022
- 490 Revelle, W. (2023), psych: Procedures for Psychological, Psychometric, and Personality Research. Northwestern University, Evanston, Illinois. R package version 2.3.6, <https://CRAN.R-project.org/package=psych>.
- Schindelegger, M., Harker, A. A., Ponte, R. M., Dobslaw, H., & Salstein, D. A. (2021). Convergence of daily GRACE solutions and models of submonthly ocean bottom pressure variability. *Journal of Geophysical Research: Oceans*, 126, e2020JC017031. <https://doi.org/10.1029/2020JC017031>
- 495 Steiger, J.H. (1980), Tests for comparing elements of a correlation matrix, *Psychological Bulletin*, 87, 245-251.

- Storto, A., S. Dobricic, S. Masina, and P. Di Pietro, 2011: Assimilating Along-Track Altimetric Observations through Local Hydrostatic Adjustment in a Global Ocean Variational Assimilation System. *Mon. Wea. Rev.*, 139, 738–754, <https://doi.org/10.1175/2010MWR3350.1>.
- 500 Storto, A., Masina, S., Balmaseda, M. et al. Steric sea level variability (1993–2010) in an ensemble of ocean reanalyses and objective analyses. *Clim Dyn* 49, 709–729 (2017). <https://doi.org/10.1007/s00382-015-2554-9>
- Storto, A.; Bonaduce, A.; Feng, X.; Yang, C. Steric Sea Level Changes from Ocean Reanalyses at Global and Regional Scales. *Water* 2019a, 11, 1987. <https://doi.org/10.3390/w11101987>
- 505 Storto A, Alvera-Azcárate A, Balmaseda MA, Barth A, Chevallier M, Counillon F, Domingues CM, Drevillon M, Drillet Y, Forget G, Garric G, Haines K, Hernandez F, Iovino D, Jackson LC, Lellouche J-M, Masina S, Mayer M, Oke PR, Penny SG, Peterson KA, Yang C and Zuo H (2019b) Ocean Reanalyses: Recent Advances and Unsolved Challenges. *Front. Mar. Sci.* 6:418. doi: 10.3389/fmars.2019.00418
- Storto, A., Masina, S., Simoncelli, S. et al. The added value of the multi-system spread information for ocean heat content and steric sea level investigations in the CMEMS GREP ensemble reanalysis product. *Clim Dyn* 53, 287–312 (2019c). <https://doi.org/10.1007/s00382-018-4585-5>
- 510 Storto, A., L. Cheng, and C. Yang, 2022: Revisiting the 2003–18 Deep Ocean Warming through Multiplatform Analysis of the Global Energy Budget. *J. Climate*, 35, 4701–4717, <https://doi.org/10.1175/JCLI-D-21-0726.1>.
- Sun, Y., P. Ditmar, and R. Riva (2016), Observed changes in the Earth's dynamic oblateness from GRACE data and geophysical models, *J. Geod.*, 90(1), 81– 89, doi:10.1007/s00190-015-0852-y.
- 515 Tapley, B.D., Bettadpur, S., Ries, J.C., Thompson, P.F. and Watkins, M.M., 2004. GRACE measurements of mass variability in the Earth system. *Science*, 305(5683), pp.503-505. DOI: 10.1126/science.1099192
- Tibshirani, R. (1997), The LASSO method for variable selection in the cox model. *Statist. Med.*, 16: 385-395. [https://doi.org/10.1002/\(SICI\)1097-0258\(19970228\)16:4<385::AID-SIM380>3.0.CO;2-3](https://doi.org/10.1002/(SICI)1097-0258(19970228)16:4<385::AID-SIM380>3.0.CO;2-3)
- Tsimplis M. N., Josey S. A. (2001). Forcing of the Mediterranean Sea by atmospheric oscillations over the north Atlantic. *Geophys. Res. Lett.* 28, 803–806. doi: 10.1029/2000GL012098
- 520 Volkov, D. L., M. Baringer, D. Smeed, W. Johns, and F. W. Landerer, 2019: Teleconnection between the Atlantic Meridional Overturning Circulation and Sea Level in the Mediterranean Sea. *J. Climate*, 32, 935–955, <https://doi.org/10.1175/JCLI-D-18-0474.1>.
- Wong, A. P. S., Wijffels, S. E., Riser, S. C., Pouliquen, S., Hosoda, S., Roemmich, D., Gilson, J., Johnson, G. C., Martini, K., Murphy, D. J., Scanderbeg, M., Bhaskar, T. V. S. U., Buck, J. J. H., Merceur, F., Carval, T., Maze, G., Cabanes, C., André, X., Poffa, N., Yashayaev, I., Barker, P. M., Guinehut, S., Belbéoch, M., Ignaszewski, M., OBaringer, M., Schmid, C., Lyman, J. M., McTaggart, K. E., Purkey, S. G., Zilberman, N., Alkire, M. B., Swift, D., Owens, W. B., Jayne, S. R., Hersh, C., Robbins, P., West-Mack, D., Bahr, F., Yoshida, S., Sutton, P. J. H., Cancouët, R., Coatanoan, C., Dobbler, D., Juan, A. G., Gourrion, J., Kolodziejczyk, N., Bernard, V., Bourlès, B., Claustre, H., Reste, F. D. S. L., Traon, P.-Y. L., Rannou, J.-P., Saout-Grit, C., Speich, S., Thierry, V., Verbrugge, N., Angel-Benavides, I. M., Klein, B., Notarstefano, G., Poulain, P.-M., Vélez-Belchí, P., Suga, T., Ando, K., Iwasaka, N., Kobayashi, T., Masuda, S., Oka, E., Sato, K., Nakamura, T., Sato, K., Takatsuki, Y., Yoshida, T., Cowley, R., Lovell, J. L., Oke, P. R., van Wijk, E. M., Carse, F., Donnelly, M., Gould, W. J., Gowers, K., King, B. A., Loch, S. G., Mowat, M., Turton, J., Rao, E. P. R., Ravichandran, M., Freeland, H. J., Gaboury, I., Gilbert, D., Greenan, B. J. W., Ouellet, M., Ross, T., Tran, A., Dong, M., Liu, Z., Xu, J., Kang, K., Jo, H., Kim, S.-D., et al.: Argo Data 1999–2019: Two Million Temperature-Salinity Profiles and Subsurface Velocity Observations From a Global Array of Profiling Floats, *Frontiers in Marine Science*, 7, <https://doi.org/10.3389/fmars.2020.00700>, 2020.
- 535

Product Ref. No	Product ID & Type	Data Access	Documentation
1	GLOBAL_REANALYSIS_PHY_001_031 (GREP), numerical models	EU Copernicus Marine Service Product (2022a)	QUID (Quality Information Document): Desportes et al. (2022) PUM (Product User Manual): Gounou et al. (2022)
2	Barystatic and manometric from satellite gravimetry (LEGOS - MAGELLIUM)	Aviso Odatis webpage, 2023: doi: 10.24400/527896/a01-2023.011	PUM (Product User Manual): https://www.aviso.altimetry.fr/fileadmin/documents/data/products/indic/WAMBOR-DT-009-MAG_CopernicusMarine_ServiceEvolution_PUM_v2.0.pdf
3	Barystatic and manometric from sea level budget (LEGOS - MAGELLIUM)	Aviso Odatis webpage, 2023: 10.24400/527896/a01-2023.012	PUM (Product User Manual): https://www.aviso.altimetry.fr/fileadmin/documents/data/products/indic/WAMBOR-DT-009-MAG_CopernicusMarine_ServiceEvolution_PUM_v2.0.pdf
4	SEALEVEL_GLO_PHY_L4_MY_008_047, L4 reprocessed altimetry observations	EU Copernicus Marine Service Product (2022b)	QUID (Quality Information Document): Pujol et al. (2023) PUM (Product User Manual): Pujol (2022)

Table 1. Product Table

Region	Trend			Seasonal amplitude			Interannual variability			Average uncertainty		
	GREP	GRAC E	SLB	GREP	GRAC E	SLB	GREP	GRAC E	SLB	GREP	GRAC E	SLB
Arctic Ocean	2.45 +/- 0.44	3.45 +/- 0.57	1.09 +/- 0.44	28.7	29.0	26.0	17.6	20.9	22.2	8.5	29.0	12.9
North Atlantic Ocean	1.81 +/- 0.18	2.67 +/- 0.23	3.24 +/- 0.16	14.4	14.2	10.7	6.1	6.0	6.6	8.0	29.9	20.8
Mediterranean Sea	1.93 +/- 0.46	0.87 +/- 0.65	2.44 +/- 0.50	30.0	31.5	25.5	20.0	27.8	29.2	13.1	31.8	11.8

545

Table 2. Manometric sea level diagnostics for the three basins considered in this study, calculated from the three datasets GREP (ensemble mean), GRACE, and SLB. The trend is calculated as a linear fit, with uncertainty found through bootstrapping. Seasonal amplitude stems from fitting the detrended timeseries to a sinusoidal line, while interannual variability is the standard deviation of the timeseries without its trend and seasonal amplitude. Average uncertainty is calculated from the gridpoint values. For GREP, it is given by the ensemble standard deviation.

550

Region	Monthly timeseries		Interannual timescale		subannual timescale	
	GRACE	SLB	GRACE	SLB	GRACE	SLB
Arctic Ocean	35%	11%	25%	11%	48%	38%
North Atlantic Ocean	56%	80%	71%	79%	34%	85%
Mediterranean Sea	4%	19%	1%	11%	8%	37%

Table 3. Percent of the regional manometric sea level variance explained by the global barystatic signal, also for the subannual and interannual signals. The global barystatic signal is shown in Figure 1 as gray lines.

555

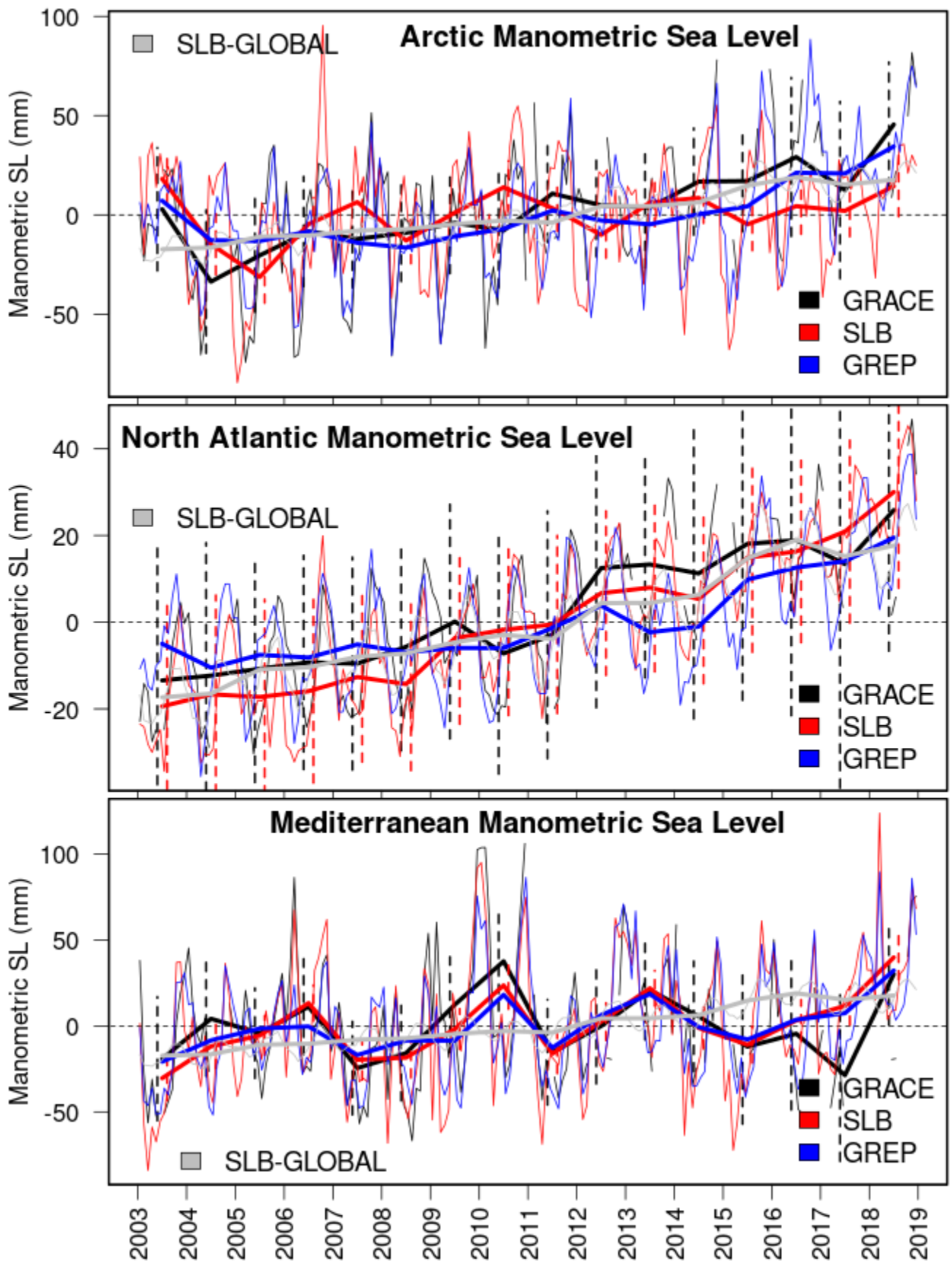
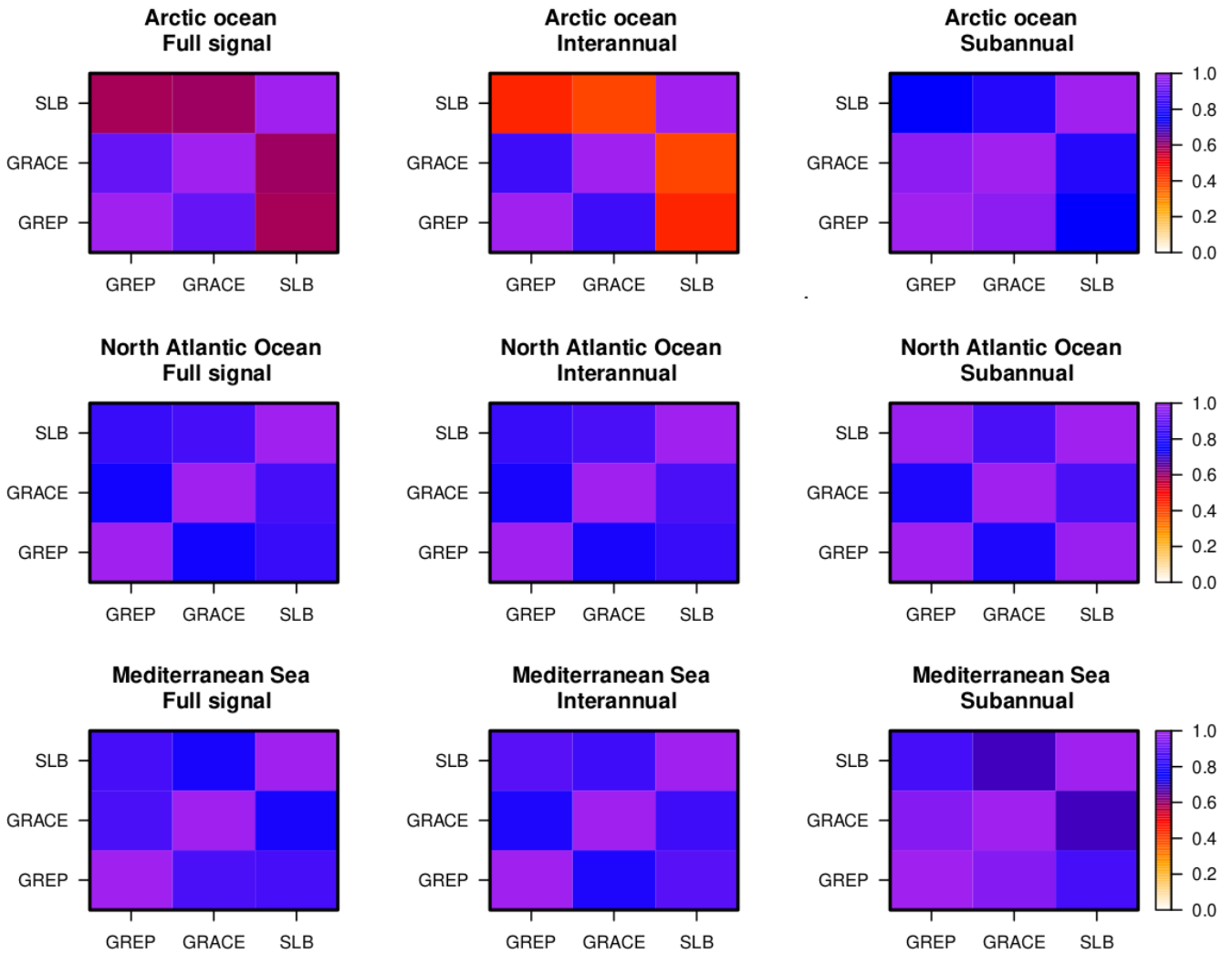


Figure 1. Manometric sea level timeseries for the Arctic, Mediterranean, and North Atlantic basins. Both monthly (thin lines) and yearly (thick lines) means are shown for GRACE, SLB, and GREP. The global barystatic sea level (SLB method) is also added in gray. The North Atlantic Ocean is defined from 0°N to 67°N , and the Arctic Ocean from 67°N in the Atlantic Ocean to the Bering Strait. Dashed vertical lines correspond to the yearly uncertainty (for GRACE and SLB only; for GREP are not shown for sake of clarity, given their underestimated value due to the small ensemble size).

560



565 **Figure 2. Correlation matrix for the three datasets in the three ocean basins investigated in this study, for both the full, the interannual, and the subannual signal. All values of correlation are statistically significant, at the 99% confidence level. Note the correlation matrix is symmetric, but all terms are shown in any case for the sake of clarity.**

570

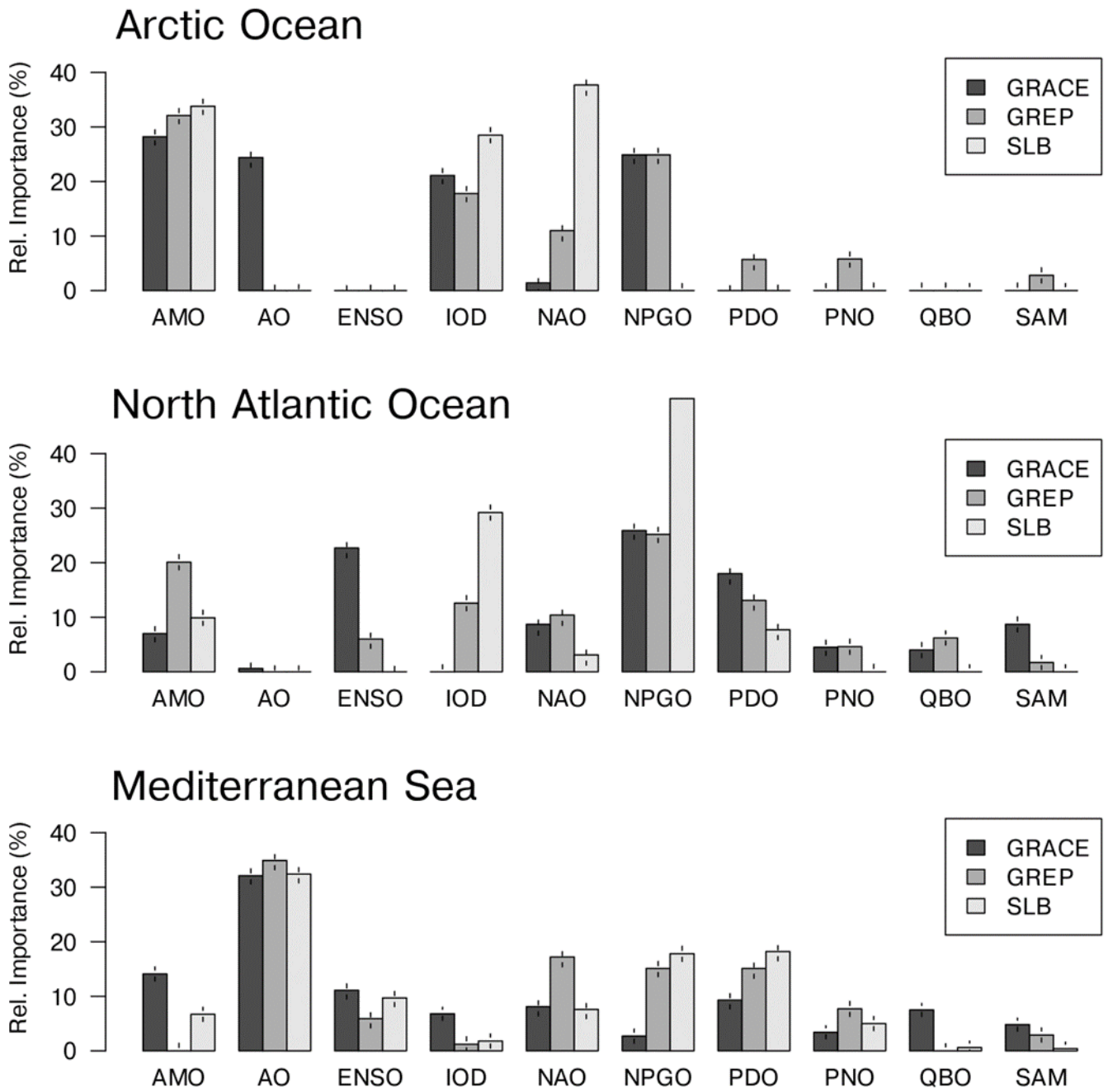


Figure 3. Relative importance (defined in the text in section 2.4) of the selected climate indices for the manometric sea level in the three basins investigated in this study, using the three datasets GRACE, GREP, and SLB. The climate indices acronyms are as follows: AMO: Atlantic Multidecadal Oscillation; AO: Arctic Oscillation; ENSO: multivariate El Niño Southern Oscillation; IOD: Indian Ocean Dipole; NAO: North Atlantic Oscillation; NPGO: North Pacific Gyre Oscillation; PDO: Pacific Decadal Oscillation; PNO: Pacific North American Oscillation; QBO: Quasi-Biennial Oscillation; SAM: Southern Annular Mode. Vertical bars indicate the regression coefficients' standard errors.